

Functional Silencing of TATA-binding Protein (TBP) by a Covalent Linkage of the N-terminal Domain of TBP-associated Factor 1^{*[5]}

Received for publication, April 9, 2007, and in revised form, June 6, 2007. Published, JBC Papers in Press, June 6, 2007, DOI 10.1074/jbc.M702988200

Tapas K. Mal[‡], Shinya Takahata^{§1}, Sewon Ki[§], Le Zheng[‡], Tetsuro Kokubo[§], and Mitsuhiro Ikura^{‡2}

From the [‡]Division of Signaling Biology, Ontario Cancer Institute, Department of Medical Biophysics, University of Toronto, Toronto Medical Discovery Towers, Toronto, Ontario M5G 1L7, Canada and the [§]Division of Molecular and Cellular Biology, International Graduate School of Arts and Sciences, Yokohama City University, 1-7-29 Suehiro-cho, Tsurumi-ku, Yokohama, Kanagawa 230-0045, Japan

General transcription factor TFIID is comprised of TATA-binding protein (TBP) and TBP-associated factors (TAFs), together playing critical roles in regulation of transcription initiation. The TAF N-terminal domain (TAND) of yeast TAF1 containing two subdomains, TAND1 (residues 10–37) and TAND2 (residues 46–71), is sufficient to interact with TBP and suppress the TATA binding activity of TBP. However, the detailed structural analysis of the complex between yeast TBP and TAND12 (residues 6–71) was hindered by its poor solubility and stability in solution. Here we report a molecular engineering approach where the N terminus of TBP is fused to the C terminus of TAND12 via linkers of various lengths containing (GGGS)_n sequence, (n = 1, 2, 3). The length of the linker within the TAND12-TBP fusion has a significant effect on solubility and stability (SAS). The construct with (GGGS)₃ linker produces the best quality single-quantum-coherence (HSQC) NMR spectrum with markedly improved SAS. In parallel to these observations, the TAND12-TBP fusion exhibits marked reduction of TBP function in binding to TAF1 as well as temperature sensitivity in *in vivo* yeast cell growth. Remarkably, the temperature sensitivity was proportional to the length of the linker in the fusions: the construct with (GGGS)₃ linker did not grow at 20 °C, while those with (GGGS)₁ and (GGGS)₂ linkers did. These results together indicate that the native interaction between TBP and TAND12 is well maintained in the TAND12-(GGGS)₃-TBP fusion and that this fusion approach provides an excellent model system to investigate the structural detail of the TBP-TAF1 interaction.

In eukaryotes, transcriptional initiation and regulation of class II genes requires a plethora of transcription factors including general transcription factors (TFIIA, TFIIB, TFIID, TFIIIE, TFIIF, and TFIIH), mediators, cofactors, chromatin modifiers, gene-specific activators and repressors, and polymerase II (1–4). In yeast, TFIID is a multisubunit general transcription factor consisting of TATA binding protein (TBP)³ and 14 TBP-associated factors (TAFs) (5, 6). TBP binds specifically to the TATA element (7), whereas TAFs bind directly and indirectly to other core promoter elements, for example the initiator and downstream promoter element (5, 8–10). In TATA-containing promoters, TAFs play an important role in facilitating transcription in response to various activators (2, 3). In many promoters including the oncogene cyclin D1, the TATA element is absent and TAFs may be more actively involved in the recruitment of TFIID to promoter sequences (11).

In *Saccharomyces cerevisiae*, TAF1 is the second largest subunit of TFIID and is thought to serve as a platform for the assembly of the whole TFIID complex (5, 6). Among the multiple TBP-binding sites of TAF1, the best characterized TAF N-terminal domain (TAND) consists of two subdomains: TAND1 (residues 10–37) and TAND2 (residues 46–71) (12–17). We have previously shown that TAND1 and TAND2 bind directly to the concave and convex surface of TBP, respectively, and thus inhibit interaction of TBP with DNA and TFIIA, thereby suppressing transcriptional activation of certain genes (13, 18–21). TAND1 also participates in transcriptional activation. In yeast cells, the deletion of TAND1 impairs the activation function of RPS5-UAS and 2× synthetic GAL4-binding sites on the RPS5 core promoter (22). Thus TAND is clearly involved in transcriptional regulation (21–24). It is interesting to note that in the absence of TBP, TAND is intrinsically disordered (Fig. 1A) (19, 20). It has recently been recognized that a large number of functional domains of eukaryotic proteins are unstructured in solution and that disordered proteins are particularly important in many key signaling pathways such as

* This project was supported in part by grants from Canadian Institutes of Health Research (to M. I.) and from the Ministry of Education, Culture, Sports, Science and Technology of Japan (to T. K.). The costs of publication of this article were defrayed in part by the payment of page charges. This article must therefore be hereby marked "advertisement" in accordance with 18 U.S.C. Section 1734 solely to indicate this fact.

[5] The on-line version of this article (available at <http://www.jbc.org>) contains supplemental Table S1 and Figs. S1 and S2.

¹ Present address: Dept. of Pathology, University of Utah, 15 N. Medical Dr. East, Salt Lake City, UT 84112.

² Holds the Canada Research Chair in Cancer Structural Biology. To whom correspondence should be addressed: Division of Signaling Biology, Ontario Cancer Institute, Dept. of Medical Biophysics, University of Toronto, Toronto Medical Discovery Towers, 101 College St., 4th floor, Rm. 804, Toronto, Ontario M5G 1L7, Canada. Tel.: 416-581-7550; Fax: 416-581-7597; E-mail: mikura@uhnres.utoronto.ca.

³ The abbreviations used are: TBP, TATA-binding protein; TAF, TBP-associated factor; TAND, TAF N-terminal domain; CFP, cyan fluorescence protein; YFP, yellow fluorescence protein; FRET, fluorescence resonance energy transfer; HSQC, heteronuclear single quantum coherence; NMR, nuclear magnetic resonance; SAS, solubility and stability; SET, solubility-enhanced tag; GST, glutathione S-transferase; IPTG, isopropyl-1-thio-β-D-galactopyranoside; CaM, calmodulin; GFP, green fluorescent protein.

Interaction between TBP and TAF1 Studied by Fusion Approach

transcriptional regulation, translation, and the cell cycle (25). These unstructured proteins or domains often undergo coupled or synergistic folding upon interaction with binding/functional partners (19, 20, 26–28). TAND12 exhibits similar behavior in the presence of TBP (Fig. 1A).

The primary sequence of the TAND region is poorly conserved between yeast and *Drosophila* (14, 29). *Drosophila* (d)TAND1 (residues 11–77) can form a stable complex with TBP, while yeast (y)TAND requires both subdomains TAND1 (residues 10–37) and TAND2 residues (46–71), and γ TAND1 is much shorter in polypeptide length compared with dTAND1 (13, 19, 20). To understand the structure function relationship of these evolutionarily diverse TAND domains in TAF1, we previously attempted detailed structural studies by NMR, but had limited success because of the poor stability and solubility (SAS) of the γ TBP and γ TAND12 complex (20).

SAS is the major obstacle for structural studies of many proteins and of their complexes in solution NMR. Structure determination by solution NMR typically requires a protein concentration of 200 μ M or greater for several days in solution. Buffer screening and point mutations have been useful to improve for the long term protein SAS in some cases (30–33). In addition, truncation or addition of a few residues at the C and N termini of the protein construct can improve SAS (26, 34). In the past, the fusion of domains has also been used for enhancing expression, SAS of proteins, as well as for studying protein-protein interactions. Wagner and co-workers (35) have introduced a solubility-enhanced tag (SET) fused to a near insoluble protein causing solubility enhancement. Green fluorescence protein (GFP) fused to the C terminus of a target protein has been used as an indicator to screen for protein folding during overexpression in micro-organisms (36). Fusion proteins have been engineered for expression of recombinant production of immunoglobulin fragments for immunological and crystallographic studies using a variety of linkers (37–43). Detailed biophysical and biochemical properties were also explored for engineered fusion proteins, for example calmodulin (CaM) fused to M13, the CaM binding region of skeletal muscle myosin light chain kinase through a glycylglycine or a GGGS pentapeptide linker (44, 45).

Here we employ a fusion approach in which the N terminus of TBP is fused with the C terminus of TAND12 via linkers (GGGS)_n of various lengths to explore whether TAND12 can regulate the function of TBP, and to facilitate NMR studies of the protein complex (Fig. 1). Our recent studies suggest that TAND of TAF1 is an autonomous regulator of TBP function (46). TAND can interact with and regulate TBP function when it is fused to either termini of any TFIID subunit. We have engineered an active fusion strategy where a linker is used to tether two interacting proteins to enhance protein-protein interaction and to improve the SAS of the complex. Three fusion constructs were made with various linker lengths and among these constructs, the fusion protein containing a (GGGS)₃ linker exhibited the greatest enhancement of SAS compared with the intermolecular complex between TBP and TAND12 (Fig. 1). The NMR data suggests that the TAND12 and TBP within the fusion protein, TAND12-(GGGS)₃-TBP form a stable intramolecular complex that mimics the native

and specific interactions observed for the intermolecular complex between TBP and TAND12. The fluorescence energy transfer (FRET) and yeast *in vivo* growth data also support this observation.

EXPERIMENTAL PROCEDURES

Plasmid Construction—pM1775 was created by disrupting the NdeI site of pM888 (TAF1/pRS314) (47) by site-directed mutagenesis (QuikChange) using the TK56 oligonucleotide. The oligonucleotides used in this study are listed in supplemental Table S1. pM4139 encoding the TAND-TBP fusion protein was constructed as follows. A DNA fragment encoding TAND (residues 8–139) was amplified by PCR with the TK4402 and TK4403 primer pair using pM1775 as a template and then inserted into the NdeI site of pM1578 (TBP/pET28a) (48). pM4139 was then subjected to site-directed mutagenesis to create pM4370 encoding TAND (residues 8–139)-(GGGS)₁-TBP (residues 61–240), using the TK6272 oligonucleotide. pM4370 was further subjected to site-directed mutagenesis to create pM4475 encoding TAND12 (residues 8–71)-(GGGS)₁-TBP, using the TK6655 oligonucleotide. pM4616 and pM4617, which encode (GGGS)₂ and (GGGS)₃ derivatives of pM4475, were created by site-directed mutagenesis using the TK7160 and TK7161 oligonucleotides, respectively. pM4754, pM4755, and pM4756, which encode TAND12 mutant derivatives of pM4475, pM4616 and pM4617, respectively, were created by site-directed mutagenesis using the TK3166 (Y19A) and TK3167 (F57A) oligonucleotides.

For the FRET experiments with YFP-TBP and GST-CFP-TAND12, pM3097 (YFP-TBP/pET28a) was constructed by inserting a DNA fragment encoding YFP into the NdeI site of pM1578, which resulted in the expression of protein having YFP fused to the N terminus of TBP. The DNA fragment encoding YFP was amplified by PCR with the TK1795 and TK1796 primer pair using pRSETb-EYFP (49, 50) as a template.

pM1683 was generated by disrupting the NdeI site and creating the NdeI/NheI sites in pM1169 (TAF1/pRS314) (12) by site-directed mutagenesis using TK56 and TK1271 oligonucleotides, respectively. The DNA fragment encoding TAND (residues 1–75) was amplified by PCR with the TK1802 and TK1423 primer pair using pM1683 as a template and then inserted into the NdeI-EcoRI sites of pET28a to create pM3098 (TAND12/pET28a). pM3099 (CFP-TAND12/pET28a) was constructed by inserting a DNA fragment encoding CFP into the NdeI site of pM3098. The DNA fragment encoding CFP was amplified by PCR with the TK1795 and TK1796 primer pair using pRSETb-ECFP (51, 52) as a template. pM3510 (GST-CFP-TAND12/pGEX-6P-1) was then constructed by inserting a DNA fragment encoding the CFP-TAND12 fusion protein into the EcoRI-XhoI sites of pGEX-6P-1 (GE Healthcare). The DNA fragment encoding the CFP-TAND12 fusion protein was amplified by PCR with the TK2210 and TK2211 primer pair using pM3099 as a template.

pM3102 (CFP-TAF1/pRS314) was constructed by ligating the NdeI fragment of pM3099 encoding CFP into the NdeI site of pM1683. pM4985 was created from pM3102 by site-directed mutagenesis using the TK311 (Y19A) and TK48 (F57A) oligonucleotides. pM7432 (GST-CFP-TAND12_{mutant}[Y19A, F57A]/

Interaction between TBP and TAF1 Studied by Fusion Approach

pGEX-6P-1) was then constructed by inserting a DNA fragment encoding the CFP-TAND12_{mutant} fusion protein into the EcoRI-XhoI sites of pGEX-6P-1. The DNA fragment encoding the CFP-TAND12_{mutant} fusion protein was amplified by PCR with the TK2210 and TK2211 primer pair using pM4985 as a template.

For the FRET experiments using CFP-TAND12-(GGGS)₃-TBP-YFP fusion proteins, pM7034 (TBP-YFP/pRS314) was constructed by inserting a DNA fragment encoding YFP, which was amplified by PCR with the TK3771 and TK3772 primer pair using pRSETb-EYFP (49, 50) as a template, into the Sall site at the C terminus of TBP encoded by pM2681 (TBP/pRS314), which is a derivative of pTM8 (48). The HindIII-XhoI fragment of pM4617 was replaced with a DNA fragment, which was amplified by PCR with the TK4000 and TK7932 primer pair using pM7034 as a template and then digested with HindIII and XhoI, to create pM7037 (TAND12-(GGGS)₃-TBP-YFP/pET28a). pM7040 (CFP-TAND12-(GGGS)₃-TBP-YFP/pET28a) was constructed by inserting a DNA fragment encoding CFP, which was amplified by PCR with the TK1795 and TK1796 primer pair using pRSETb-ECFP (51, 52) as a template, into the NdeI site of pM7037. M7430 was created from pM7040 by inserting a short DNA fragment encoding Strep tag just before the stop codon of YFP by site-directed mutagenesis using TK9422 oligonucleotide.

For expression of TAND12-TBP fusion proteins in yeast cells, pM1482 was constructed by inserting a DNA fragment encoding seven repeats of the FLAG epitope tag into the Sall site at the N terminus of TBP encoded by pM1481 (TBP/pRS314), which is a derivative of pTM8 (48). pM1615 was constructed by inserting a DNA fragment encoding TAND (8–96 amino acids), which was amplified by PCR with the TK1198 and TK1199 primer pairs using pM1775 as a template, into the Sall site of pM1482 (FLAG-tagged TBP/pRS314). pM1615 was then subjected to site-directed mutagenesis to create pM3671 encoding FLAG-tagged TAND12 (residues 8–71)-TBP, using the TK2480 oligonucleotide. pM4700, pM4701 and pM4702, which encode FLAG-tagged TAND12 (residues 8–71)-(GGGS)_n-TBP ($n = 1, 2, \text{ and } 3$), were constructed by replacing the BssHII-BalI fragment of pM3671 with the corresponding BssHII-BalI fragments of pM4475, pM4616, and pM4617, respectively. pM4757, pM4758, and pM4759, which encode TAND mutant derivatives of pM4700, pM4701, and pM4702, respectively, were created by site-directed mutagenesis using the TK3166 (Y19A) and TK3167 (F57A) oligonucleotides. pM1481 was subjected to site-directed mutagenesis to create pM4080 encoding TBP, using the TK3620 oligonucleotide. pM4872 (FLAG-tagged TBP/pRS314) was constructed by replacing the Sall-BamHI fragment of pM3671 with the Sall-BamHI fragment of pM4080.

Protein Expression and Purification—The protocol for obtaining *Saccharomyces cerevisiae* TAF1 (yTAND12) and TBP (yTBP) proteins have been described elsewhere (20). Briefly, TAND12 was expressed with a GST affinity tag while TBP was His₆-tagged. These proteins were purified with glutathione-Sepharose (GE Healthcare) and Ni-NTA affinity columns, respectively. They were further purified by size exclusion gel filtration column using Superdex 75 (GE Healthcare). Two

samples for the TBP-TAND12 complex were prepared, each with one component being uniformly ¹⁵N labeled.

Three fusion constructs were transformed into BL21(DE3) codon plus (Stratagene). Cells were grown at 37 °C until an A_{600} of 1.0 and induced with 0.5 mM isopropyl- β -D-thiogalactopyranoside (IPTG) at 15 °C overnight. The His-tagged proteins were lysed by sonication and bound to Ni-NTA agarose (Qiagen) in buffer-1 containing 20 mM Tris-HCl, pH 7.5, 10% glycerol, 100 mM KCl, 12.5 mM MgCl₂, 0.2 mM EDTA, 1 mM dithiothreitol, 0.1% Nonidet P-40, protease inhibitor (Roche Applied Science). After washing with five column volumes with buffer-2 (buffer 1 with 20 mM imidazole), the bound proteins were cut from Ni-NTA beads by overnight treatment with thrombin in the same buffer at 4 °C. After thrombin cleavage, the fusion proteins were passed through an ion exchange using a Hi Trap column (GE Healthcare) employing a linear salt gradient of buffer-3 (50 mM glycine pH 9.0, 5% glycerol, 5 mM dithiothreitol, 1 mM phenylmethylsulfonyl fluoride) and buffer-4 (Buffer 3 + 1 M KCl) and were eluted at a salt concentration of 150 mM KCl. They were further purified by using a Superdex 75 size exclusion column in a buffer containing 20 mM Hepes, 120 mM KCl, 5 mM MgCl₂, 5% glycerol, 2 mM Tris (2-carboxyethyl) phosphine hydrochloride (TCEP) at pH 7.0. The yield of these fusion constructs were as follows: TAND12-(GGGS)₁-TBP, 6 mg/liter; TAND12-(GGGS)₂-TBP, 8 mg/liter, and TAND12-(GGGS)₃-TBP, 9 mg/liter. Isotope-labeled protein samples were obtained by bacterial expression in modified minimal M9 medium supplemented with 1 g/liter [¹⁵N]ammonium chloride as sole source of ¹⁵N and/or 2 g/liter D-[¹³C]glucose and 100% ²H₂O.

The plasmids encoding the GST-CFP-TAND12 fusion protein (pM3510) or its TAND12 mutant derivative (pM7432) were transformed into BL21 (DE3) pLysS (Invitrogen). Cells were grown in LB medium containing ampicillin (50 μ g/ml) at 37 °C until A_{600} 0.6 and then expression was induced by adding IPTG to 0.5 mM. After 3 more hours of incubation at the same temperature the cells were lysed by sonication, and the GST-tagged protein was bound to glutathione-Sepharose in buffer 5 containing 25 mM Hepes-KOH (pH 7.6), 100 mM KCl, 10% (v/v) glycerol, 0.1 mM EDTA, 1 mM dithiothreitol, and 0.1% Nonidet P-40. After extensive washing with buffer 5, the bound proteins were eluted with buffer 6 (buffer 5 with 10 mM glutathione) and dialyzed against buffer-7 containing 50 mM Tris-HCl (pH 7.5), 150 mM KCl, 10% (v/v) glycerol, 0.2 mM EDTA, 1 mM dithiothreitol, 1 mM phenylmethylsulfonyl fluoride, and 12.5 mM MgCl₂ for the FRET experiments.

The plasmid encoding the YFP-TBP fusion protein (pM3097) was transformed into BL21 (DE3) pLysS (Invitrogen). Cells were grown in LB medium containing kanamycin (50 μ g/ml) at 30 °C until A_{600} 0.6 and then expression was induced by adding IPTG to 0.5 mM. After 3 more hours of incubation at the same temperature, the cells were lysed by sonication, and the His-tagged protein was bound to Ni-NTA agarose in buffer 8 containing 40 mM Tris-HCl (pH 7.5), 500 mM KCl, 10% (v/v) glycerol, 0.2 mM EDTA, 1 mM dithiothreitol, and 10 mM imidazole. After extensive washing with buffer 8, the bound proteins were eluted with buffer 9 (buffer 8 with 100 mM imidazole) and dialyzed against buffer 7 for the FRET experiments.

Interaction between TBP and TAND1 Studied by Fusion Approach

The plasmid encoding CFP-TAND12-(GGGS)₃-TBP-YFP fusion protein (pM7040) was transformed into BL21 Star (DE3) pLysS (Invitrogen). Cells were grown in LB medium containing kanamycin (50 μg/ml) at 18 °C for 2 days without addition of IPTG. The His- and Strep-tagged proteins were lysed by sonication and bound to Ni-NTA agarose in buffer-10 containing 40 mM Tris-HCl (pH 7.5), 200 mM KCl, 10% (v/v) glycerol, 0.2 mM EDTA, 1 mM dithiothreitol, and 10 mM imidazole. After extensive washing with buffer 10, the bound proteins were eluted with buffer 11 (buffer 10 with 100 mM imidazole). Eluted fractions were further purified by StrepTactin Superflow Agarose (Novagen) chromatography according to the manufacturer's protocol and used for the FRET experiments.

Preparation of TBP-γTAND12 Complex—The TBP-TAND12 complex was prepared by slow addition of purified TBP protein solution at low concentration (<0.3 mg/ml) to TAND12 in the presence of 120 mM KCl. Unlabeled protein concentration was always used in excess. The mixed solution was concentrated and applied to a Superdex-75 size exclusion column to separate uncomplexed protein and other impurities from the complex in buffer solution of 20 mM Hepes (pH 7.0), 5% glycerol, 2 mM TCEP, 10 mM MgCl₂, 0.02 mM NaN₃. The collected sample was then passed through a Mono-S column for final purification and the complex was concentrated using a centricon-10 (Amicon) for NMR and solubility test.

Yeast Strains, Media, and Cultures—Standard techniques were used for yeast growth and transformation. YAK303 (48) was used as the host strain in the plasmid shuffle experiments. Briefly, it was transformed with pM4872, pM4700, pM4701, pM4702, pM4757, pM4758, or pM4759. Transformants were spotted on 5-fluoroorotic acid (5-FOA)-containing plates, and then cultured at several different temperatures for 3–5 days.

GST Pull-down Assay—The GST pull-down experiments were conducted as described previously (14), with the exception that the TBP and GST-TAND proteins were detected by immunoblotting.

Fluorescence Spectroscopy—The fluorescence spectra were recorded on a fluorescence spectrophotometer RF-5300PC (Shimadzu, Japan) using a 3-mm path-length quartz microcuvette at room temperature. The fluorescence emission was monitored between 450 and 600 nm with excitation at 437 nm. The measurements were performed using ~5 μg (supplemental Fig. S1A) or 15 (supplemental Fig. S1B) of purified fusion proteins in 300 μl of buffer 6. In the supplemental Fig. S1B, the spectrum was also measured after trypsin treatment (1 mg/ml, 5 min at room temperature).

Hanging Drop Stability and Solubility Test—Stability and solubility (SAS) test was done for the TBP-TAND12 complex and the fusion TAND12-(GGGS)₃-TBP protein using a hanging-drop technique with a 24-well VDX plate (Hampton Research). SAS was screened at two different protein concentrations (1 mM and 0.5 mM). Every drop contains 3 μl of protein sample. The mother liquid contains 1 ml of buffer containing 20 mM Hepes, 120 mM KCl, 5% glycerol, 2 mM TCEP, 10 mM MgCl₂. The drops were observed under a Nikon microscope, and images were taken every other day.

NMR Spectroscopy—NMR samples of uniformly ¹⁵N-labeled TAND12-(GGGS)₁-TBP, TAND12-(GGGS)₂-TBP, and

TAND12-(GGGS)₃-TBP fusion constructs were prepared in 20 mM Hepes pH 7.0, 5% deuterated glycerol, 120 mM KCl, 10 mM MgCl₂, 2 mM TCEP, 0.02 mM NaN₃, and 90% H₂O/10% ²H₂O (v/v) buffer with a concentration of 0.6–0.8 mM. For peptide backbone assignments of the TAND12-(GGGS)₃-TBP protein, a triple-labeled, ²H,¹⁵N,¹³C sample was prepared for HNCA/HNCOCA and HN(CA)CB/HN(COCA)CB experiments. NMR samples of the intermolecular TBP-TAND12 complex comprised of one ¹⁵N-labeled and one unlabeled protein were used for ¹H-¹⁵N heteronuclear single quantum coherence (HSQC) experiments in the same buffer as the fusion constructs. All NMR experiments were performed at 25 °C on a Varian Inova 600 MHz spectrometer equipped with a triple resonances pulse field gradient cold probe. ¹H-¹⁵N HSQC spectra were recorded with 128 and 576 complex points in *t*₁ and *t*₂, respectively. Spectral width were 34 ppm and 15 ppm for the ¹⁵N (*F*₁) and ¹H (*F*₂) dimension, respectively. NMR data were processed and analyzed using NMRPipe/NMRDraw (53) and XEasy (54).

RESULTS

Fusion Constructs Design and Production—The fusion constructs were designed to have a linker of the minimal length that would allow TBP and TAND12 to interact in a manner that mimics the native structural and functional properties of the intermolecular TBP-TAND12 complex. We have taken advantage of a previously determined solution structure of TBP in complex with *Drosophila* TAF N-terminal domain 1 (dTAND1, residues 11–77) and other previous structural and biochemical reports on the design of fusion constructs (12, 18–20). In the structure of TBP-dTAND1, dTAND1 occupies the concave surface of TBP structure and both the N and C termini of dTAND1 are projected away from the termini of TBP (Fig. 1). Our previous structural and mutation studies suggest that γTAND1 and γTAND2 interact with the concave and convex surfaces of the saddle-like structure of TBP, respectively. In addition, the convex γTAND2 interacting surface is close to the N terminus of TBP. Based on these results, we have constructed three different fusion constructs by fusing the N terminus of TBP to the C terminus of TAND12 using linkers of various length (GGGS)_{*n*}, *n* = 1, 2, 3 to produce TAND12-(GGGS)₁-TBP, TAND12-(GGGS)₂-TBP, and TAND12-(GGGS)₃-TBP (Fig. 1B). The fusion constructs were subsequently cloned, expressed and purified as described under “Experimental Procedures.” All fusion constructs expressed well and were purified to >95% homogeneity.

In Vitro and in Vivo Characterization of TAND12 and TBP Interactions in the Fusion Protein—To confirm that TAND12 binds to TBP within the fusion protein in a manner analogous to the native complex of TAND12 and TBP proteins, the three fusion proteins described above were subjected to GST pull-down assays and FRET analysis. In the pull-down experiment, if TAND12 and TBP formed an intra-molecular complex within the fusion protein, the fusion protein would not bind to exogenously added GST-TAND12 and, therefore, would not be trapped by glutathione-Sepharose beads. This was indeed the case (lanes 7–9 in Fig. 2). In contrast, fusion proteins carrying two amino acid substitutions (Y19A and F57A) in the TAND12

Interaction between TBP and TAF1 Studied by Fusion Approach

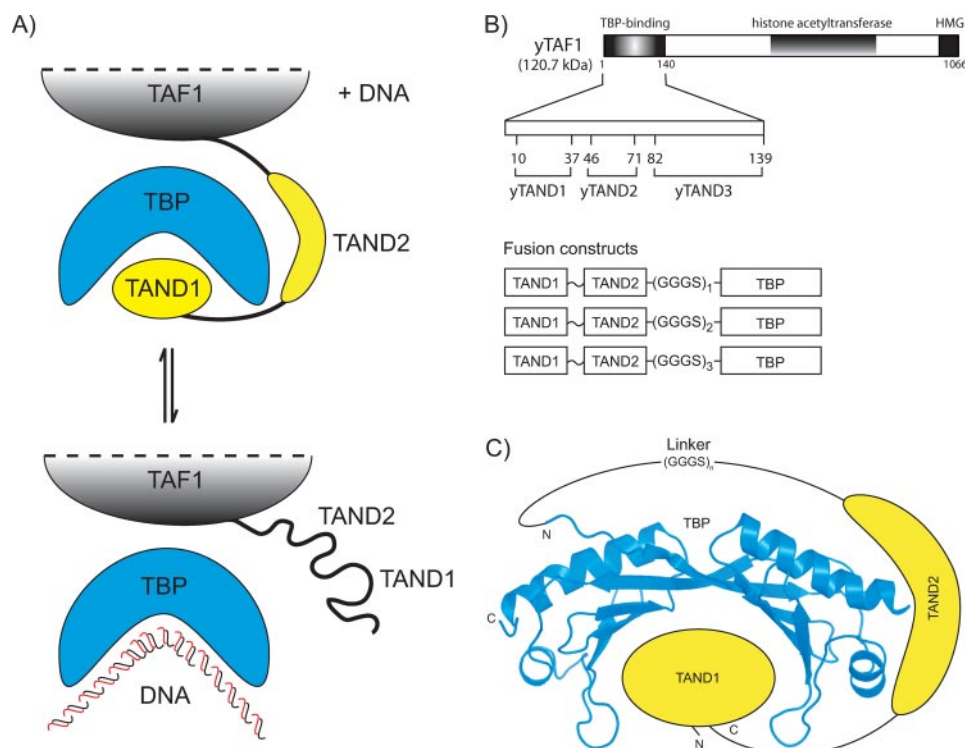


FIGURE 1. Schematic diagrams representing induced folding and strategy for fusion constructs. *A*, schematic of coupled folding of the two N-terminal subdomains of yTAF1 (TAND12). The structured TANDs are shown in yellow, whereas unstructured TANDs are represented by a black line; the rest of TAF1 is represented in gray and TBP in blue. TAND1 and TAND2 interact with concave and convex surfaces of TBP, respectively. In the absence of TBP, TAND1 and TAND2 are unstructured. *B*, schematic representation of domain architecture of yTAF1. The yTAF1 N-terminal domain (TAND) can be subdivided into three subdomains (yTAND1, yTAND2, and yTAND3). Schematic representation of fusion constructs: TAND12 and TBP are shown in rectangles. GGGGS is used as a linker between TAND12 and TBP for fusion purposes. *C*, schematic diagram of fusion construct design. TBP was fused to the C terminus of TAND through one to three GGGGS linkers. The TBP ribbon structure is shown in blue, and TAND1 and TAND2 are shown in yellow and linker (GGGS)_n, n = 1, 2, 3 is shown as a solid line between N terminus of TBP and C terminus of TAND2. TBP structure was drawn using PyMol software (available at www.pymol.org).

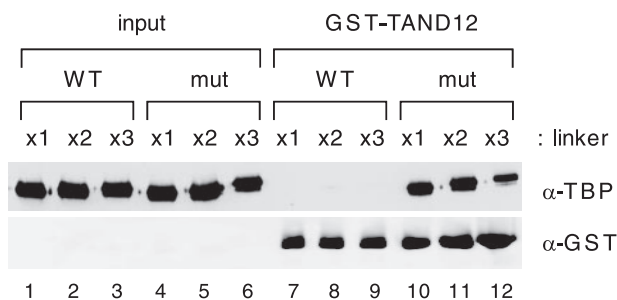


FIGURE 2. Pull-down assay of TAND-TBP fusion proteins. The TBP core domain (residues 61–240) fused to intact TAND12 (indicated as WT, lanes 1–3 and 7–9) or mutant TAND12 (Y19A/F57A, indicated as mut, lanes 4–6 and 10–12) via different GGGGS linkers (repeat number; ×1, ×2, ×3), or the GST-tagged TAND12 protein (GST-TAND12), were expressed in *Escherichia coli*. Bacterial cell lysates containing equimolar amounts of TBP derivatives or GST-TAND12 were mixed together and then passed through glutathione-Sepharose resin. Complexes bound to the resin were eluted and resolved by SDS-PAGE. The lysates of TBP derivatives corresponding to 100% of input were separated on the same gel to provide a positional marker and a loading control (lanes 1–6). Samples were transferred to a nitrocellulose membrane and probed with anti-TBP (upper panel) or anti-GST (lower panel) polyclonal antibodies.

domain, which are known to substantially diminish the interaction with TBP, were subjected to the same assay and did bind to exogenously added GST-TAND12 (lanes 10–12 in Fig. 2). These data indicate that the TBP within the fusion protein is

functional, at least in TAND12 binding. Unfortunately, this experiment was not sensitive enough to differentiate the effect of linker length on the intramolecular interaction between TAND12 and TBP, because all three of the intact proteins displayed similar interactions with the exogenously added GST-TAND12. Nevertheless, this result confirms that the interaction between wild-type TAND12 and TBP in the fusion constructs is not constrained by linker lengths.

To probe intermolecular interactions between TAND12 and TBP in the fusion proteins, we employed FRET spectroscopy (55, 56). TAND12 and TBP were fused with a cyan fluorescent protein (CFP) (51, 52) and a yellow fluorescent protein (YFP) (49, 50), respectively (described under “Experimental Procedures”). The resulting two fusion proteins, *i.e.* CFP-TAND12 and YFP-TBP, were expressed, purified, and then mixed together to test whether FRET occurs when they are together in solution. The fluorescence spectrum was monitored between 450 and 600 nm with excitation at 437 nm when CFP-TAND12 was alone or mixed with YFP-TBP. Under

these conditions, efficient FRET (intensity ratio of emission at 526 and 476 nm) was observed specifically when the two proteins were mixed (supplemental Fig. S1A). Importantly, when CFP-TAND12_{mutant} (Y19A, F57A) was mixed with YFP-TBP, the FRET signal was significantly weaker than when CFP-TAND12 was used, confirming that FRET was a consequence of an interaction between TAND12 and TBP (supplemental Fig. S1A).

Subsequently, we produced the protein CFP-TAND12-(GGGS)₃-TBP-YFP by fusing CFP and YFP to the N terminus and C terminus of TAND12-(GGGS)₃-TBP, respectively (described under “Experimental Procedures”) (supplemental Fig. S1B), and this fusion protein exhibited a much stronger FRET signal as compared with that of the CFP-TAND12 and YFP-TBP complex. Furthermore, this FRET signal was abolished by proteolytic treatment with trypsin, a protease that cleaves the polypeptide chain between CFP and YFP (*i.e.* TAND12-(GGGS)₃-TBP) but leaves CFP and YFP unaffected (57) (supplemental Fig. S1B). These results clearly show that TAND12 and TBP interact intramolecularly with even greater efficiency when fused together than when they are separate proteins. It is also noteworthy to mention that we attempted FRET experiments with CFP-TAND12_{mutant}-(GGGS)₃-TBP-YFP as well as with the other two fusion constructs; CFP-

Interaction between TBP and TAF1 Studied by Fusion Approach

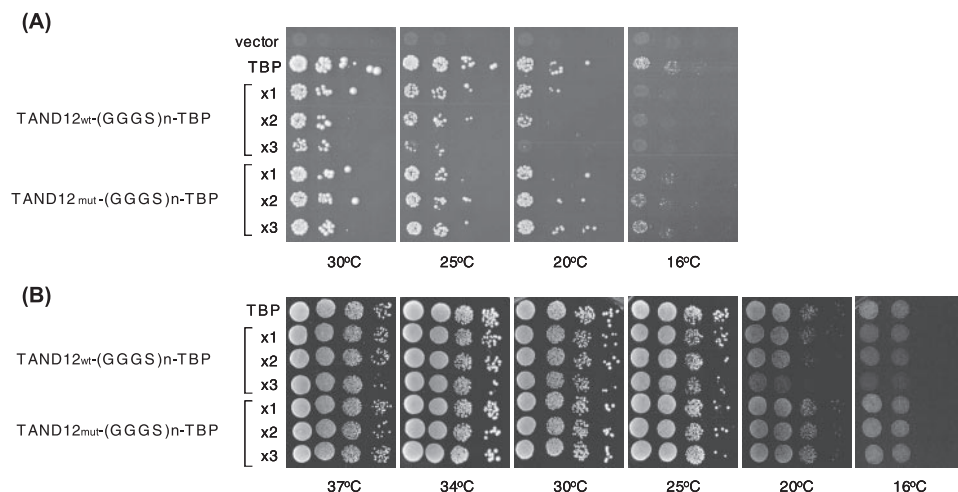


FIGURE 3. *In vivo* characterization of TAND12-TBP fusion proteins. *A*, yeast strains expressing wild-type TBP from the *URA3*-marked plasmid (*top line*, indicated as *vector*) together with one of the TBP derivatives (core domain, residues 61–240) alone, or fused to intact or mutant TAND12 via GGGG linkers of different lengths (repeat number; $\times 1$, $\times 2$, $\times 3$) as shown at the *left*, from the *TRP1*-marked plasmid were serially diluted 10-fold, spotted onto 5-fluoroorotic acid (5-FOA) containing medium, and grown at the indicated temperatures for 3–5 days. *B*, yeast strains isolated from the plate incubated at 30 °C in *A* were serially diluted 10-fold, spotted onto YPD medium, and grown at the indicated temperatures for 3–5 days.

TAND12-(GGGS)₁-TBP-YFP and CFP-TAND12-(GGGS)₂-TBP-YFP. However, all of these constructs were very prone to proteolytic cleavage and hence could not be purified as intact proteins (data not shown). This observation strongly suggests that TBP and TAND12 do not form a stable complex within these fusion proteins, which makes them very susceptible to degradation. Collectively, the results of the FRET analysis demonstrate that the (GGGS)₃ linker between TBP and TAND12 in the fusion stabilizes the formation of an intramolecular complex that is similar to the intermolecular one formed between TBP and TAND12.

We further investigated whether the TBP within the fusion protein remained functional with regard to properties other than TAND12 binding. A yeast strain carrying the *TBP* gene on a *URA3*-marked plasmid instead of on the chromosome was transformed with *TRP1*-marked plasmids encoding TBP alone, or encoding one of the fusion proteins bearing intact or mutant TAND12, and the transformed yeast were then tested for growth on 5-FOA containing medium (Fig. 3A). If yeast strains could survive on this medium, TBP expressed from the *TRP1*-marked plasmid should be functional in transcription mediated not only by pol II but also by pol I and III. The results indicated that TBP in the fusion proteins was functional at 30 °C, irrespective of linker length or of whether TAND12 was wild-type or mutant (compare the lower six lines with the upper two, *i.e.* negative (vector) and positive (TBP) controls in Fig. 3A). Intriguingly, yeast strains expressing intact TAND12 fusions did not grow well at 16 °C while those expressing the TAND12 mutant derivatives grew at levels similar to the strain expressing TBP alone. Furthermore, the strain expressing TAND12wt-(GGGS)₃-TBP did not grow at 20 °C, but strains expressing TAND12wt-(GGGS)₁-TBP or TAND12wt-(GGGS)₂-TBP were able to grow. In contrast, there was no such linker length effect observed for strains expressing TAND mutant derivatives. Collectively, these results indicate that a stable interaction between TAND12 and TBP within the fusion protein occurs at

lower temperatures and is favored by extending the linker length. This observation was further confirmed by testing the growth phenotypes of yeast strains that had survived on 5-FOA medium at 30 °C (Fig. 3A) on rich medium at several different temperatures (Fig. 3B). Again, the linker length effect was observed at lower temperatures only in those strains expressing fusions with wild-type TAND12 sequences.

NMR Characterization of TAND12-(GGGS)_n-TBP Fusion—These fusion constructs were screened by solution NMR to determine whether any produce spectra of sufficient quality for structural studies. All proteins were expressed in M9 medium using ¹⁵N-labeled NH₄Cl as the sole source of nitrogen and purified to >95% homogeneity as

determined by SDS-PAGE and mass spectroscopy (data not shown). ¹H-¹⁵N HSQC data were recorded on all three fusion proteins (Fig. 4). The quality of the ¹H-¹⁵N HSQC spectra improved with increasing GGGG linker length with the TAND12-(GGGS)₃-TBP fusion construct producing the best spectrum. The spectrum of the TAND12-(GGGS)₁-TBP fusion was of poor quality. However, it was interesting to note that the line widths were broader than those constructs with longer linkers. This suggests that one GGGG linker is not long enough to initiate substantial intra-molecular interaction between TAND12 and TBP, and perhaps they remain largely as two independent entities in solution around the linker. As previously observed, TBP is not stable *in vitro* in the absence of a binding partner and readily comes out of solution, either by dimerization or aggregation (24). On the other hand TAND12 is unfolded on its own, and undergoes induced folding upon binding to TBP (20). Therefore, it is not surprising that the fusion protein, TAND12-(GGGS)₁-TBP readily comes out of solution within a couple of hours. The fusion construct TAND12-(GGGS)₂-TBP produced a better spectrum, though it still contains a number of broadened resonances and several very intense signals between 7.5–8.0 ppm, probably originating from unstructured residues in the GGGG linker region. This result indicates that the linker is just long enough to introduce constraint and intermittent interaction between TAND12 and TBP, but not sufficiently long enough to allow a stable intramolecular interaction. Nevertheless, the construct was stable and stayed in solution longer than TAND12-(GGGS)₁-TBP fusion protein. These results strongly suggest that the length of the linker is a key factor for the enhanced SAS and the quality of NMR spectrum of the fusion proteins.

Comparison of SAS Studies of TAND12-(GGGS)₃-TBP and TAND12-TBP Complex—Our previous attempt on the structural study of TBP-yTAND12 complex was hindered due to its poor SAS. The complex was stable for 2 days at most and steadily came out of solution under the NMR condition used

Interaction between TBP and TAF1 Studied by Fusion Approach

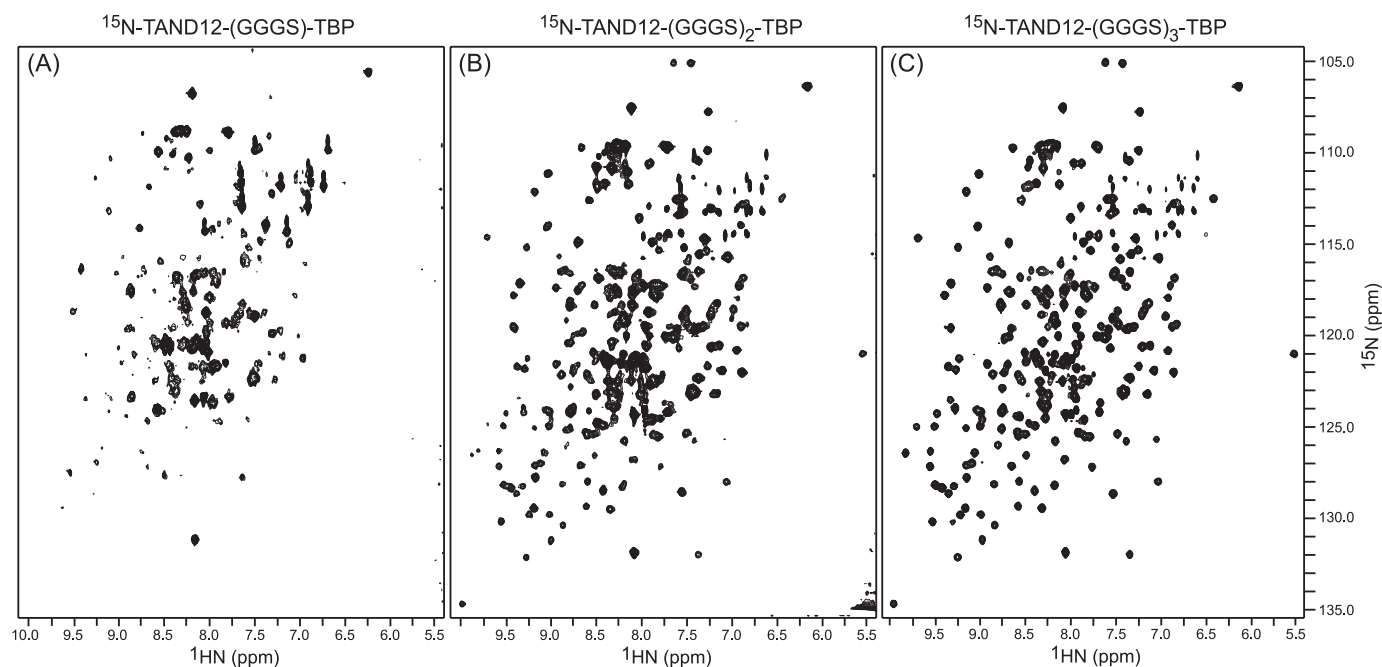


FIGURE 4. ^1H - ^{15}N HSQC spectra of fusion constructs and SAS test. ^1H - ^{15}N HSQC spectrum of uniformly ^{15}N -labeled samples of three fusion construct. A, TNAD12-(GGGS)₁-TBP. B, TNAD12-(GGGS)₂-TBP. C, TNAD12-(GGGS)₃-TBP.

(20). Out of three constructs, because the TAND12-(GGGS)₃-TBP fusion produced the best quality spectrum, we decided to test long term SAS to assess the feasibility of performing detailed structural studies of this construct by solution NMR. SAS studies were performed on both the TAND12-(GGGS)₃-TBP fusion protein and the complex of TBP-TAND12 in a buffer condition identical to that used for NMR experiments (20 mM Hepes pH 7.0, 5% deuterated glycerol, 120 mM KCl, 10 mM MgCl₂, 2 mM Tris(2-carboxyethyl) phosphine (TCEP), 0.02 mM NaN₃) at 25 °C using the hanging drop technique commonly used for crystallography screening. Under this condition, we screened for precipitation every other day under a microscope. As previously observed, the intermolecular complex started coming out of solution from the second day and considerable precipitation was observed on the fourth day. On the other hand, the fusion protein remained in solution over 2 weeks without any traces of precipitation (supplemental Fig. S2).

Identification of Slow Exchange Amide Protons in TAND12-(GGGS)₃-TBP Fusion—With all the structural and functional analyses on these three fusion constructs as described above, we have decided to further characterize the TAND12-(GGGS)₃-TBP fusion protein by NMR spectroscopy. We recorded ^1H - ^{15}N HSQC spectrum on an uniformly triple-labeled ^2H , ^{13}C , ^{15}N TAND12-(GGGS)₃-TBP and compared it with that of TBP-TAND12 complex (Fig. 5). The HSQC spectrum of this fusion is almost identical to a summation of two ^1H - ^{15}N HSQC spectra obtained from TBP-TAND12 complexes in which each subunit was individually ^{15}N -labeled. One significant difference was the presence of a few additional resonances that were attributed to the three repeat GGGS linker residues. However, a large number of the assignments could easily be transferred from TBP-TAND12 complex. These assignments were later confirmed by recording transverse relaxation optimized spectroscopy (TROSY)-based triple resonance three-dimensional

HNCA, HN(CO)CA, HN(COCA)CB and HN(CA)CB data (58–60) of TAND12-(GGGS)₃-TBP fusion. The remaining resonances were subsequently assigned using these data sets. The similarity in the spectral data strongly suggests that the structure of the fusion TAND12-(GGGS)₃-TBP protein is nearly identical to the intermolecular complex between TBP and TAND12 proteins.

Because the fusion TAND12-(GGGS)₃-TBP protein was produced in 100% $^2\text{H}_2\text{O}$ M9 medium, not all exchangeable deuterons were substituted with protons even after passing through an ion exchange column at pH 9.0 during the course of purification (see under “Experimental Procedures.”) In the fusion protein, a number of residues from TBP are protected for several days from H/D exchange, including Val⁷¹, Ala⁷², Ile¹⁰³, Met¹⁰⁴, Ala¹¹³, Leu¹¹⁴, Ile¹¹⁵, Phe¹¹⁶, Met¹²¹, Val¹²², Val¹²³, Thr¹²⁴, Val²⁰³, Leu²⁰⁴, and Leu²⁰⁵ (Fig. 6A). These data provide a valuable information on the structural stability of the TAND12-(GGGS)₃-TBP fusion protein. The protected residues were mapped on the structure of TBP and were found to be located at two distinct areas of the TBP saddle structure (Fig. 6B). First, we find that the major part of the concave surface of TBP is highly protected. Remarkably, this site coincides with our previous observation from chemical shift perturbation studies mapping TAND12 interaction sites on TBP (20). Therefore, it is likely that the exchangeable amide deuteron of these residues are shielded from solvent by TAND1, thereby, protecting from H/D exchange. Second, the C-terminal α -helix 2 on the convex surface of TBP also exhibited H/D protection with residues including Ala¹³⁵, Tyr¹³⁹, and Ile¹⁴³. However, no H/D protection was observed for the equivalent helix (α -helix 2') on the other half of the 2-fold symmetrical structure of TBP. Interestingly, this asymmetric H/D protection is in good agreement with our previous report which mapped the TAND2 interaction site on helix-2 using chemical shift perturbation (Fig. 6)

Interaction between TBP and TAF1 Studied by Fusion Approach

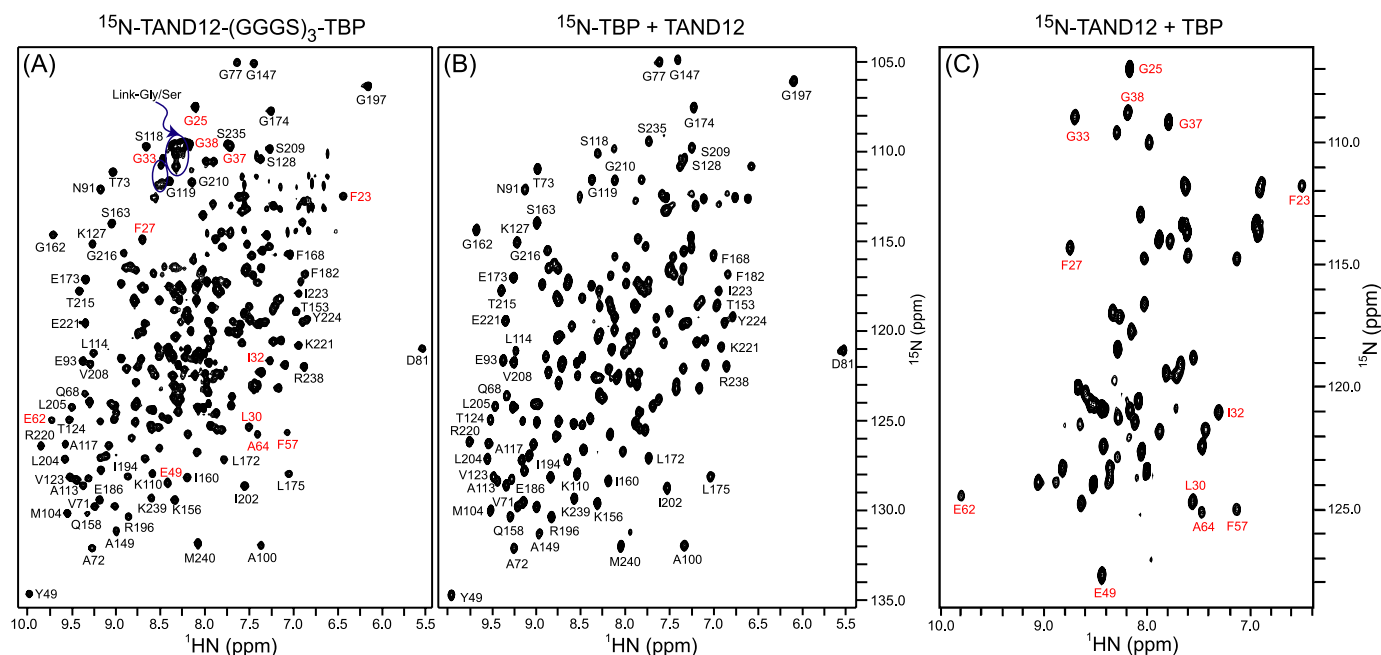


FIGURE 5. Comparison of ^1H - ^{15}N HSQC spectra between fusion constructs and TBP-TAND12 complex. ^1H - ^{15}N HSQC spectra of fusion constructs of uniformly ^{15}N labeled (A) TAND12-(GGGS) $_3$ -TBP, (B) TBP in complex with unlabeled TAND12, and (C) TAND12 in complex with unlabeled TBP. For clarity, only a few assigned resonances were marked with residue numbers in each spectrum. To distinguish resonances between the TAND12 and TBP components of the fusion protein, assignments for residues from TAND12 are shown in red while those for TBP are shown in black.

(20). It is noteworthy to mention here that this asymmetric interaction of TAND2 with TBP is driven by electrostatic interaction because γ TAND2 is enriched with acidic residues and helix-2 of TBP contains a number of basic residues while helix 2' has no basic residue (20). Therefore, it is evident from this result that TAND2 masks the C-terminal part of helix 2 of TBP from H/D exchange. Together these results demonstrate that TBP and TAND12 within the fusion form a stable and tight complex mimicking the native interactions between TBP and TAND12 complex.

DISCUSSION

We previously reported that TAND of TAF1 could act independently from the rest of the molecule (46). The functional autonomy of TAND was tested by fusing it to the N or C termini of several other components of TFIID and it was found to have similar function as at the N terminus of TAF1. However, it lost its autonomy when it was fused at the termini of other components of the preinitiation complex. Functionally, TAF1 gene lacking TAND resulted in a temperature-sensitive growth phenotype that could largely be rescued by fusing TAND to the termini of any component of TFIID. This result suggested that the TBP binding activity of TAND was essential for growth at restrictive temperature and could modulate the TBP-TATA interaction independent of the other domains of TFIID. The present work not only supports our previous study on the autonomous function of TAND from TAF1 but also provides a new avenue to structurally characterize the TBP-TAF1 interaction in detail.

The observation that TAND12-TBP fusion proteins can support normal growth of yeast cells at 30 °C, or higher temperatures, indicates that TBP within these proteins is folded in a native conformation, albeit with the TAND12 domain present

at the N terminus. These data are consistent with results obtained from *in vitro* studies, *i.e.* GST pull-down assays, FRET analysis and NMR data. In particular, FRET provided evidence for spatial proximity between the N terminus of TAND12 and the C terminus of TBP within the fusion protein, and that was abolished by proteolytic treatment with trypsin. In *in vivo* assays, only the fusion proteins bearing the wild-type TAND12 sequence conferred a cold-sensitive growth phenotype and this effect was strengthened by increased linker length. As all of these fusion proteins were expressed at similar levels *in vivo* (data not shown), it is likely that TAND12 binds to TBP more stably at lower temperatures when connected by a linker of appropriate length, in this case the twelve-amino acid (GGGS) $_3$ linker. These functional results clearly indicate that the fusion construct TAND12-(GGGS) $_3$ -TBP is capable of suppressing TBP function. These data confirm us that the functional integrity of TBP and TAND12 is preserved in the fusion system. Moreover, the fusion system is superior in terms of SAS compared with the native TBP-TAND12 complex as described below.

There have been tremendous developments in NMR methodology and instrumentation as well as sample preparation procedures in the last decades. Recent introduction of cryo-probes and high field magnets over 18.8 Tesla have improved resolution and sensitivity, and that reduces the requirement of sample concentration to ~ 0.2 mM. Often proteins require high salt to improve their solubility, and that drastically reduces the sensitivity gain achievable by cryo-probe. In many biological applications, it is still a major challenge to obtain a good biomolecular sample that can stay in solution for a longer period of time and produce good NMR data for detailed structural characterization of protein-protein complexes. A major obstacle

Interaction between TBP and TAF1 Studied by Fusion Approach

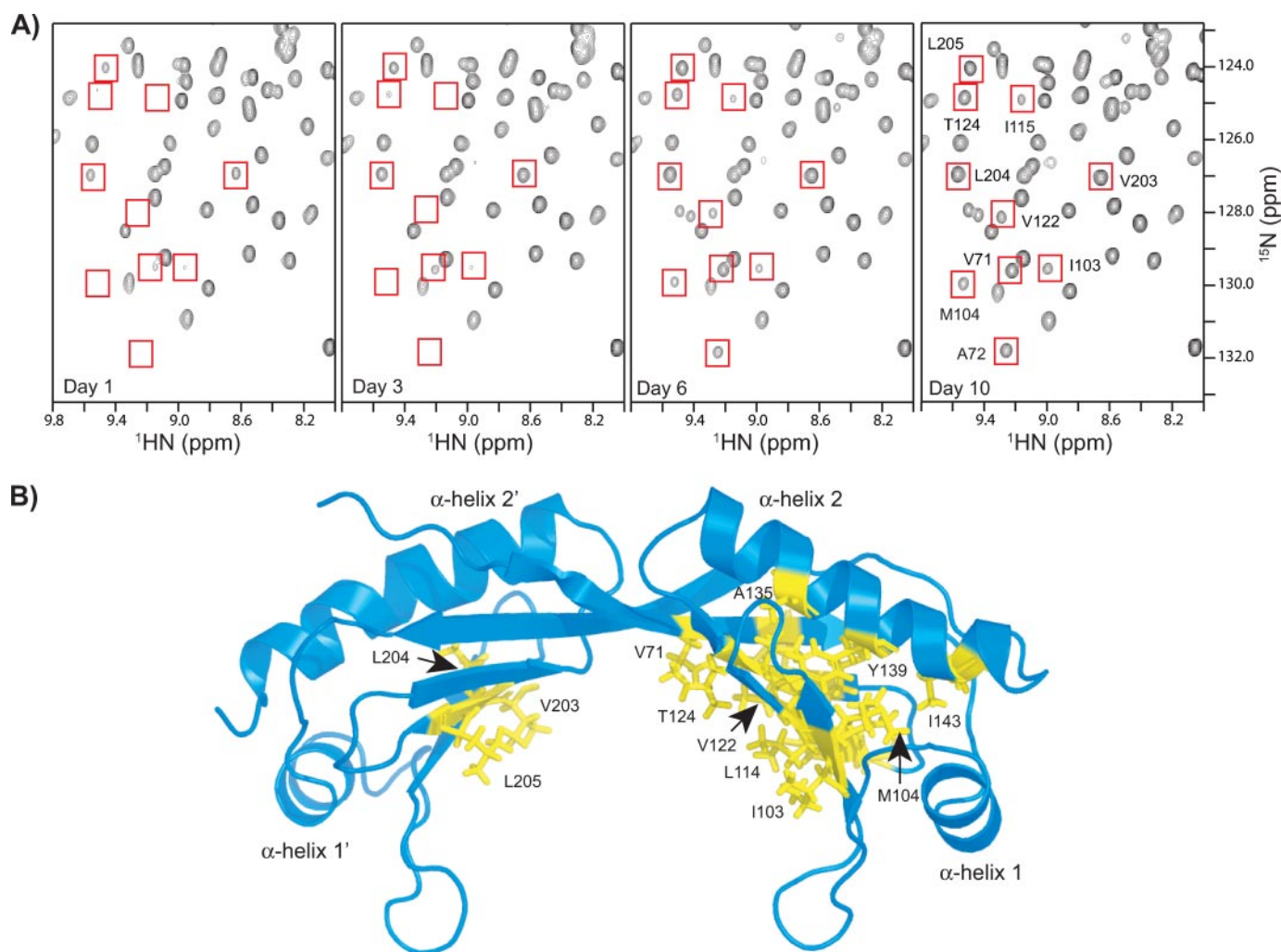


FIGURE 6. H/D exchange and mapping of protected residues on TBP structure. *A*, part of ^1H - ^{15}N HSQC spectra of the uniformly triple-labeled ^2H , ^{13}C , ^{15}N -TAND12-(GGGS) $_3$ -TBP fusion protein sample recorded 1, 3, 6, and 10 days after purification in $^1\text{H}_2\text{O}$ buffer to monitor H/D protection of exchangeable amide deuterium are shown. Resonances corresponding to residues exhibiting H/D protection for several days are boxed with red rectangles and labeled with their residue type and numbers. *B*, residues exhibiting H/D protection are mapped on the TBP ribbon structure shown in blue drawn using PyMol software. H/D protected residues are illustrated with yellow side chains and only a few residues are labeled for clarity.

stems from the fact that protein tends to associate and aggregate at the high concentration required for NMR data collection. In the past, fusion proteins have been used for various applications including crystallography, fluorescence and imaging studies. Though fusion proteins are routinely used for affinity purification and SAS, usually fusion tags are removed for structural and functional studies. A recently introduced solubility-enhanced tag (SET), a small protein fused to a protein of interest, has been shown to markedly improve solubility (35). The fusion of SET can be regarded as a passive fusion approach because the fusion tag was not actively involved in the protein-protein interaction, but was present only to enhance the solubility of the protein of interest. In our present study, we have employed an active fusion strategy that has not only enhanced SAS, but also mimics the interaction of the native complex between TBP and TAND12. In addition the active fusion strategy effectively increases local protein concentration by augmenting the encounter rate between the two interacting proteins, thereby increasing the population of protein-protein complex formation. This strategy can also be particularly useful

for the study of low affinity protein-protein/peptide complexes *in vitro*.

γ TAF1 is a large \sim 120-kDa protein with multiple functional regions including a putative histone acetyltransferase domain, a HMG promoter binding domain, and binding sites for other TFIID subunits including TBP (61). Unfortunately, the protein is too large to be easily amenable for NMR analysis in complex with TBP. Hence we have followed truncation approach by dissecting the N-terminal TBP binding domain of TAF1 which has made it feasible to elucidate the structure of TBP- γ TAF1 complex. Our previous observation suggests that γ TAND domain requires both subdomains (TAND1 and TAND2) to form a stable complex with TBP: γ TAND1 or γ TAND2 alone does not bind TBP at high affinity. This synergistic binding of both subdomains is required to inhibit TBP-TATA interaction (14) and we therefore decided to perform structural studies on the interactions between TBP and TAND12. However, our previous attempt to perform detailed structural characterization of the TBP-TAND12 complex was not successful due to the poor SAS of this complex (20). In the present study, we engineered an

active fusion protein connected by a GGGs linker that improved SAS markedly. Because we did not have prior information about the optimal length of the linker, we made three fusion constructs using various linker lengths. The TAND12-(GGGS)₃-TBP protein produced the best ¹H-¹⁵N HSQC spectrum which was very similar to the combined spectra of individually ¹⁵N-labeled TBP-TAND12 complex. In addition, our *in vitro* FRET studies strongly suggest that the affinity of the interaction between TAND12 and TBP is much stronger in the fusion TAND12-(GGGS)₃-TBP protein than in the complex consisting of individual proteins. Furthermore, *in vivo* yeast growth functional studies indicate that the TAND12-(GGGS)₃-TBP produced the highest cold-sensitive growth phenotype. Together with *in vivo* and *in vitro* studies confirm that this fusion construct mimics the native interaction between TBP and TAND12 with individual functional integrity.

We have demonstrated that the fusion approach markedly improves the long term SAS of TAND12 and TBP complex within the fusion protein and has made it possible to aim for the detailed structural investigation of this complex by solution NMR. It is noteworthy to mention that the length of the linker is an important factor to have optimal native-like interaction. In order to optimize SAS, a number of constructs should be made and be tested with functional properties for validation. The generated TBP-TAND12 fusion system and its concept offer new opportunities (i) to suppress TBP activity in transcription initiation in cell-based experiments and (ii) to probe the interaction between TBP and TAF1 upon various types of cellular stimulus. The methodology may also enable us to investigate the interaction of TBP with other transcriptional activators such as VP16, which has low affinity toward TBP. Fusing VP16 with TAND2 in a similar manner may allow us to observe the interaction of VP16 with the TBP concave surface. More recently, we have shown that an additional segment adjacent to TAND2, named TAND3 (residues 82–139), also contribute to TBP binding and stimulates transcription activation when fused to GAL4 DNA-binding domain in a similar manner to yTAND1 (12). Collectively, TAND maintains TBP in an inactive state until it encounters an activation signal from activator. The mechanism underlying the activator-dependent activation of TBP in the TATA promoter recognition is still largely ill-defined. The present study will greatly help to understand the dynamic nature of these interactions in detail and to dissect the contribution of individual domains to the formation of a stable yTAF1 and TBP complex.

Acknowledgments—We thank Robert Roeder for providing the original vector for TBP expression. We also thank Setsuko Tomita and Hidei Ryu for constructing several plasmids used in the FRET study. We also thank Chris Marshall for thorough reading and critical comments on this manuscript and Noboru Ishiyama for helping to create the TBP figure in PyMol.

REFERENCES

- Orphanides, G., Lagrange, T., and Reinberg, D. (1996) *Genes Dev.* **10**, 2657–2683
- Roeder, R. G. (1998) *Cold Spring Harb. Symp. Quant. Biol.* **63**, 201–218
- Naar, A. M., Lemon, B. D., and Tjian, R. (2001) *Annu. Rev. Biochem.* **70**, 475–501
- Lee, T. I., and Young, R. A. (2000) *Annu. Rev. Genet.* **34**, 77–137
- Sanders, S. L., Garbett, K. A., and Weil, P. A. (2002) *Mol. Cell. Biol.* **22**, 6000–6013
- Tora, L. (2002) *Genes Dev.* **16**, 673–675
- Patikoglou, G. A., Kim, J. L., Sun, L., Yang, S. H., Kodadek, T., and Burley, S. K. (1999) *Genes Dev.* **13**, 3217–3230
- Butler, J. E., and Kadonaga, J. T. (2002) *Genes Dev.* **16**, 2583–2592
- Burke, T. W., and Kadonaga, J. T. (1997) *Genes Dev.* **11**, 3020–3031
- Chalkley, G. E., and Verrijzer, C. P. (1999) *EMBO J.* **18**, 4835–4845
- Hilton, T. L., and Wang, E. H. (2003) *J. Biol. Chem.* **278**, 12992–13002
- Takahata, S., Ryu, H., Ohtsuki, K., Kasahara, K., Kawaichi, M., and Kokubo, T. (2003) *J. Biol. Chem.* **278**, 45888–45902
- Kokubo, T., Swanson, M. J., Nishikawa, J. I., Hinnebusch, A. G., and Nakatani, Y. (1998) *Mol. Cell. Biol.* **18**, 1003–1012
- Kotani, T., Miyake, T., Tsukihashi, Y., Hinnebusch, A. G., Nakatani, Y., Kawaichi, M., and Kokubo, T. (1998) *J. Biol. Chem.* **273**, 32254–32264
- Martel, L. S., Brown, H. J., and Berk, A. J. (2002) *Mol. Cell. Biol.* **22**, 2788–2798
- Banik, U., Beechem, J. M., Klebanow, E., Schroeder, S., and Weil, P. A. (2001) *J. Biol. Chem.* **276**, 49100–49109
- Bai, Y., Perez, G. M., Beechem, J. M., and Weil, P. A. (1997) *Mol. Cell. Biol.* **17**, 3081–3093
- Bagby, S., Mal, T. K., Liu, D., Raddatz, E., Nakatani, Y., and Ikura, M. (2000) *FEBS Lett.* **468**, 149–154
- Liu, D., Ishima, R., Tong, K. I., Bagby, S., Kokubo, T., Muhandiram, D. R., Kay, L. E., Nakatani, Y., and Ikura, M. (1998) *Cell* **94**, 573–583
- Mal, T. K., Masutomi, Y., Zheng, L., Nakata, Y., Ohta, H., Nakatani, Y., Kokubo, T., and Ikura, M. (2004) *J. Mol. Biol.* **339**, 681–693
- Chitkila, C., Huisinga, K. L., Irvin, J. D., Basehoar, A. D., and Pugh, B. F. (2002) *Mol. Cell* **10**, 871–882
- Cheng, J. X., Floer, M., Ononaji, P., Bryant, G., and Ptashne, M. (2002) *Curr. Biol.* **12**, 1828–1832
- Kobayashi, A., Miyake, T., Kawaichi, M., and Kokubo, T. (2003) *Nucleic Acids Res.* **31**, 1261–1274
- Kou, H., Irvin, J. D., Huisinga, K. L., Mitra, M., and Pugh, B. F. (2003) *Mol. Cell. Biol.* **23**, 3186–3201
- Dyson, H. J., and Wright, P. E. (2005) *Nat Rev Mol. Cell. Biol.* **6**, 197–208
- Radhakrishnan, I., Perez-Alvarado, G. C., Parker, D., Dyson, H. J., Montminy, M. R., and Wright, P. E. (1997) *Cell* **91**, 741–752
- Uesugi, M., Nyanguile, O., Lu, H., Levine, A. J., and Verdine, G. L. (1997) *Science* **277**, 1310–1313
- Kussie, P. H., Gorina, S., Marechal, V., Elenbaas, B., Moreau, J., Levine, A. J., and Pavletich, N. P. (1996) *Science* **274**, 948–953
- Nishikawa, J., Kokubo, T., Horikoshi, M., Roeder, R. G., and Nakatani, Y. (1997) *Proc. Natl. Acad. Sci. U. S. A.* **94**, 85–90
- Lepre, C. A., and Moore, J. M. (1998) *J. Biomol. NMR.* **12**, 493–499
- Howe, P. W. (2004) *J. Biomol. NMR.* **30**, 283–286
- Ducat, T., Declerck, N., Gostan, T., Kochoyan, M., and Demene, H. (2006) *J. Biomol. NMR.* **34**, 137–151
- Bagby, S., Tong, K. I., and Ikura, M. (2001) *Methods Enzymol.* **339**, 20–41
- Radhakrishnan, I., Perez-Alvarado, G. C., Parker, D., Dyson, H. J., Montminy, M. R., and Wright, P. E. (1999) *J. Mol. Biol.* **287**, 859–865
- Zhou, P., Lugovskoy, A. A., and Wagner, G. (2001) *J. Biomol. NMR.* **20**, 11–14
- Waldo, G. S., Standish, B. M., Berendzen, J., and Terwilliger, T. C. (1999) *Nat. Biotechnol.* **17**, 691–695
- Huston, J. S., Levinson, D., Mudgett-Hunter, M., Tai, M. S., Novotny, J., Margolies, M. N., Ridge, R. J., Brucoleri, R. E., Haber, E., Crea, R., and Oppermann, H. (1988) *Proc. Natl. Acad. Sci. U. S. A.* **85**, 5879–5883
- Hebell, T., Ahearn, J. M., and Fearon, D. T. (1991) *Science* **254**, 102–105
- Glockshuber, R., Malia, M., Pfitzinger, I., and Pluckthun, A. (1990) *Biochemistry* **29**, 1362–1367
- Dal Porto, J., Johansen, T. E., Catipovic, B., Parfiit, D. J., Tuveson, D., Gether, U., Kozlowski, S., Fearon, D. T., and Schneck, J. P. (1993) *Proc. Natl. Acad. Sci. U. S. A.* **90**, 6671–6675
- Hoedemaeker, F. J., Signorelli, T., Johns, K., Kuntz, D. A., and Rose, D. R.

Interaction between TBP and TAF1 Studied by Fusion Approach

- (1997) *J. Biol. Chem.* **272**, 29784–29789
42. Trinh, R., Gurbaxani, B., Morrison, S. L., and Seyfzadeh, M. (2004) *Mol. Immunol.* **40**, 717–722
43. Volkman, B. F., Prehoda, K. E., Scott, J. A., Peterson, F. C., and Lim, W. A. (2002) *Cell* **111**, 565–576
44. Martin, S. R., Bayley, P. M., Brown, S. E., Porumb, T., Zhang, M., and Ikura, M. (1996) *Biochemistry* **35**, 3508–3517
45. Porumb, T., Yau, P., Harvey, T. S., and Ikura, M. (1994) *Protein Eng.* **7**, 109–115
46. Takahata, S., Kasahara, K., Kawaichi, M., and Kokubo, T. (2004) *Mol. Cell. Biol.* **24**, 3089–3099
47. Kasahara, K., Kawaichi, M., and Kokubo, T. (2004) *Genes Cells* **9**, 709–721
48. Kobayashi, A., Miyake, T., Ohyama, Y., Kawaichi, M., and Kokubo, T. (2001) *J. Biol. Chem.* **276**, 395–405
49. Heim, R., Cubitt, A. B., and Tsien, R. Y. (1995) *Nature* **373**, 663–664
50. Cormack, B. P., Valdivia, R. H., and Falkow, S. (1996) *Gene (Amst.)* **173**, 33–38
51. Heim, R., Prasher, D. C., and Tsien, R. Y. (1994) *Proc. Natl. Acad. Sci. U. S. A.* **91**, 12501–12504
52. Heim, R., and Tsien, R. Y. (1996) *Curr. Biol.* **6**, 178–182
53. Delaglio, F., Grzesiek, S., Vuister, G. W., Zhu, G., Pfeifer, J., and Bax, A. (1995) *J. Biomol. NMR* **6**, 277–293
54. Bartels, C. H., Xia, T.-H., Billeter, M., Guntert, P., and Wuthrich, K. (1995) *J. Biomol. NMR* **5**, 1–10
55. Zhang, J., Campbell, R. E., Ting, A. Y., and Tsien, R. Y. (2002) *Nat. Rev. Mol. Cell. Biol.* **3**, 906–918
56. Truong, K., and Ikura, M. (2001) *Curr. Opin. Struct. Biol.* **11**, 573–578
57. Miyawaki, A., Llopis, J., Heim, R., McCaffery, J. M., Adams, J. A., Ikura, M., and Tsien, R. Y. (1997) *Nature* **388**, 882–887
58. Gardner, K. H., and Kay, L. E. (1998) *Annu. Rev. Biophys. Biomol. Struct.* **27**, 357–406
59. Yang, D. S., and Kay, L. E. (1999) *J. Am. Chem. Soc.* **121**, 2571–2575
60. Pervushin, K., Riek, R., Wider, G., and Wuthrich, K. (1997) *Proc. Natl. Acad. Sci. U. S. A.* **94**, 12366–12371
61. Irvin, J. D., and Pugh, B. F. (2006) *J. Biol. Chem.* **281**, 6404–6412